Archived at the Flinders Academic Commons:

http://dspace.flinders.edu.au/dspace/

The following article appeared as:

Bissett, M.A., Barlow, A.J., Shapter, J.G. and Quinton, J.S., 2011. Transition from single to multi-walled carbon nanotubes grown by inductively coupled plasma enhanced chemical vapor deposition. Journal of Applied Physics, 110, 034301.

and may be found at:

http://jap.aip.org/resource/1/japiau/v110/i3/p034301_s1

DOI: http://dx.doi.org/10.1063/1.3615945

Transition from single to multi-walled carbon nanotubes grown by inductively coupled plasma enhanced chemical vapor deposition

Mark A. Bissett, Anders J. Barlow, Joe G. Shapter, and Jamie S. Quinton

Related Articles

Magnetic and electrical properties of PbTiO3/Mn-Zn ferrite multiphase nanotube arrays by electro-deposition
J. Appl. Phys. 112, 104310 (2012)

Note: Axially pull-up electrochemical etching method for fabricating tungsten nanoprobes with controllable aspect ratio
Rev. Sci. Instrum. 83, 106109 (2012)

Effects of carbon nanofillers on enhancement of polymer composites
J. Appl. Phys. 112, 074302 (2012)

Improving the field emission of carbon nanotubes by lanthanum-hexaboride nano-particles decoration
Appl. Phys. Lett. 101, 123116 (2012)

Catalyst-free synthesis of reduced graphene oxide–carbon nanotube hybrid materials by acetylene-assisted annealing graphene oxide
Appl. Phys. Lett. 101, 123107 (2012)

Additional information on J. Appl. Phys.

Journal Homepage: http://jap.aip.org/

Journal Information: http://jap.aip.org/about/about_the_journal

Top downloads: http://jap.aip.org/features/most_downloaded

Information for Authors: http://jap.aip.org/authors

Transition from single to multi-walled carbon nanotubes grown by inductively coupled plasma enhanced chemical vapor deposition

Mark A. Bissett, Anders J. Barlow, Joe G. Shapter, and Jamie S. Quinton[a)]
Smart Surface Structures Group, Centre for Nanoscale Science and Technology, School of Chemical and Physical Sciences, Flinders University, Bedford Park, Adelaide, South Australia, 5042

In this work a simple and up-scalable technique for creating arrays of high purity carbon nanotubes via plasma enhanced chemical vapor deposition is demonstrated. Inductively coupled plasma enhanced chemical vapor deposition was used with methane and argon mixtures to grow arrays in a repeatable and controllable way. Changing the growth conditions such as temperature and growth time led to a transition between single and multi-walled carbon nanotubes and was investigated. This transition from single to multi-walled carbon nanotubes is attributed to a decrease in catalytic activity with time due to amorphous carbon deposition combined with a higher susceptibility of single-walled nanotubes to plasma etching. Patterning of these arrays was achieved by physical masking during the iron catalyst deposition process. The low growth pressure of 100 mTorr and lack of reducing gas such as ammonia or hydrogen or alumina supporting layer further show this to be a simple yet versatile procedure. These arrays were then characterized using scanning electron microscopy, Raman spectroscopy and x-ray photoelectron spectroscopy. It was also observed that at high temperature (550 °C) single-walled nanotube growth was preferential while lower temperatures (450 °C) produced mainly multi-walled arrays. © *2011 American Institute of Physics*. [doi:10.1063/1.3615945]

I. INTRODUCTION

Carbon nanotubes (CNTs) are a unique material with many varied applications in the electronics industry such as field emission,[1] electrochemical sensors,[2,3] and photovoltaics.[4–6] However, one hindrance to their wide-scale implementation is the ability to produce them both cheaply and with a well-defined structure, both physical and electronic. Current synthesis techniques include arc discharge,[7] laser ablation,[8] and chemical vapor deposition[9] (CVD), with CVD being the most promising approach for high yields. CVD has the benefit of producing the nanotubes directly on a substrate making integration into devices much easier than solution processing of CNTs. An extension to CVD, plasma-enhanced CVD (PECVD) offers several advantages over thermal CVD such as the use of low pressure environments, aiding cleanliness and meaning that much lower concentrations of reactants can be used, while the plasma state aids dissociation of the feedstock gas affording lower temperature processes to be used, and therefore a wider range of substrates.[10–12] While the plasma typically contains a carbon feedstock gas such as methane or acetylene, it also often consists of a reducing gas such as hydrogen or ammonia. In the case of hydrogen this has been found to aid in the carbon feedstock dissociation and also affect the catalyst activity.[13,14]

Although PECVD has been studied extensively the production of single-walled carbon nanotubes (SWCNTs) remains more difficult to achieve than multi-walled nanotubes (MWCNTs).[12,15,16] It has been shown previously that the CNTs can be tailored by altering growth conditions such as the catalyst material and thickness, plasma composition and power, and the growth temperature.[12,17] Low temperatures tend to favor production of MWCNT and high temperature tending toward SWCNT.[12,18]

For any wide-scale device implementation the selectivity of nanotube type is paramount. One easy way to analyze grown CNTs is with Raman spectroscopy. CNTs have many specific peaks in their Raman spectra that can be used to identify them as either SWCNT or MWCNT and also be used as a measure of defects.[19] The main peaks of interest are the RBM or radial breathing mode which is caused by circumferential phonon interaction. The position of this peak is directly proportional to the diameter of the nanotube. The D band or disorder band is caused by disruptions to the electronic density of states of the nanotube. The G band or graphitic band is caused by sp^2 hybridized carbon present in graphite and CNTs. The ratio of disorder to graphitic carbon (D/G ratio) can be used as a measure of CNT purity, pristine SWCNT nanotubes should have very little to no D band, whereas MWCNT will have very high D band intensity.

Here Raman spectroscopy is used to analyze CNTs grown by PECVD and show that by altering the synthesis variables such as growth time and growth temperature that SWCNT or MWCNT can be selectively produced and patterned with exceptional homogeneity across a large area. The transition from single to multi-walled structures with changing growth time and temperature is investigated. The low pressure used for growth, 100 mTorr, allows for cheap up-scaling while the lack of both an alumina underlay and a reducing gas also reduces overall costs and simplifies the growth procedure.

II. EXPERIMENTAL DETAILS

Nanotube growth was performed in a radio-frequency (13.56 MHz) inductively coupled plasma system with a base

---

a)Author to whom correspondence should be addressed. Electronic mail: Jamie.Quinton@flinders.edu.au.
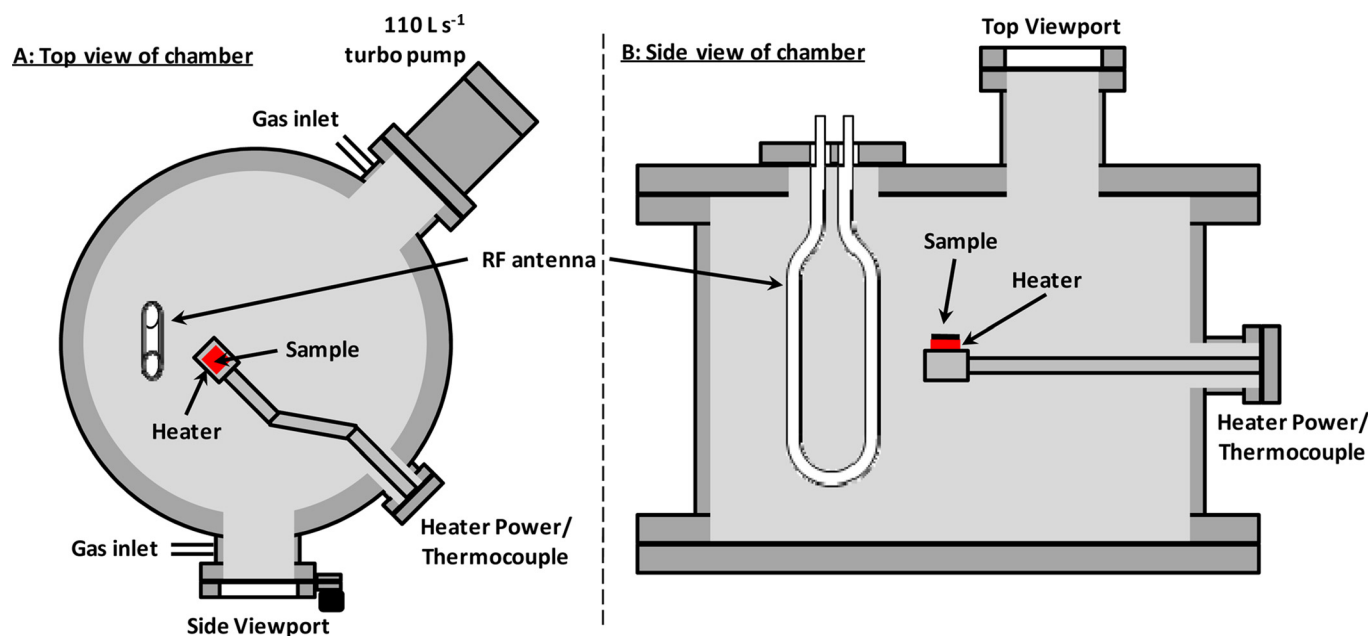
FIG. 1. (Color online) Reaction chamber used in this research showing (A) top view and (B) side view. In (B) the antenna is shown rotated 90° for clarity. Distance between antenna and sample is 10 cm.

pressure of 10^{-6} Torr, shown in Fig. 1. In this work, boron doped p-type silicon wafers ($\langle 100 \rangle$, 0.0008–0.0012 Ω cm, Siltronix, France) were used as substrates. Silicon provides excellent thermal stability and the native oxide present on the surface (SiO_2) also assists in CNT growth by inhibiting the diffusion of catalyst atoms into the substrate.[20] A 5 nm thick layer of 99.998% iron (Koch-Light Laboratories) was deposited onto the silicon substrate using a commercial sputter coater (Quorumtech K575X, Quorum Technologies, UK). The thickness was measured by an *in situ* quartz crystal microbalance. By masking areas of the substrate it is possible to investigate the difference between areas where catalyst has been deposited and the masked areas of bare substrate. Substrates were heated to 450–650 °C as specified via a resistive heating element embedded within the sample table, and left to equilibrate for 10 min. The carbon feedstock gas used was high purity methane, it has been shown previously that pure methane needs to be diluted to achieve CNT growth.[21] Neutrals such as nitrogen and argon plasma help to remove any amorphous carbon produced during growth, leading to a high purity and homogenous CNT array.[12,21,22] As mentioned previously typically hydrogen is added into the growth mixture, however, in this work this was found to not be necessary and this is believed to be due to the large number of dissociation products available from a methane plasma, listed in Table I, which show that molecular hydrogen can be supplied by the methane itself.

In this work methane was diluted with high purity argon. Once the sample is thermally stable the gas mixture is introduced to provide a total pressure of 100 mTorr in a 1:4 ratio (CH_4:Ar). The plasma is then ignited at 10 W total power and growth is undertaken for 10, 30, and 60 min as specified after which the plasma was turned off and the sample left to cool to room temperature under vacuum.

Synthesized CNT arrays were analyzed using scanning electron microscopy (SEM) (Camscan MX2500, CamScan Electron Optics Limited, UK) using a secondary electron detector. The electron source was a tungsten filament and the accelerating voltage used was 10 kV. Prior to imaging each sample was sputter coated with 10 nm of platinum using a Quorumtech K575X (Quorum Technologies, UK).

The chemical environment of the substrates was analyzed using x-ray photoelectron spectroscopy (XPS). The XPS setup used in this work was a Leybold-Heraeus LHS-10, in a chamber with a base pressure of 10^{-9} Torr and an operating pressure of 10^{-8} Torr. The source was a dual anode x-ray source (Specs, Germany) and the energy used was Al Kα (1486.6 eV) with a 20 eV pass energy. Survey spectra were taken in constant retarding ratio mode, while high resolution spectra were an average of five spectra taken in fixed analyzer transmission mode.

Confocal Raman spectroscopy was used to investigate the structure of the produced CNT arrays. Raman measurements in this work were taken on an alpha300R microscopy/spectroscopy setup (Witec, Germany) using a 532 nm laser with a maximum power of 65 mW. For each single spectrum an integration time of 6 seconds was used with ten iterations. For image spectra, where the size is mentioned next to the appropriate figure, 2500 spectra with an integration time of 0.5 s and 50×50 points per image was used. The spectra

TABLE I. Methane dissociation reactions (Ref. 23).

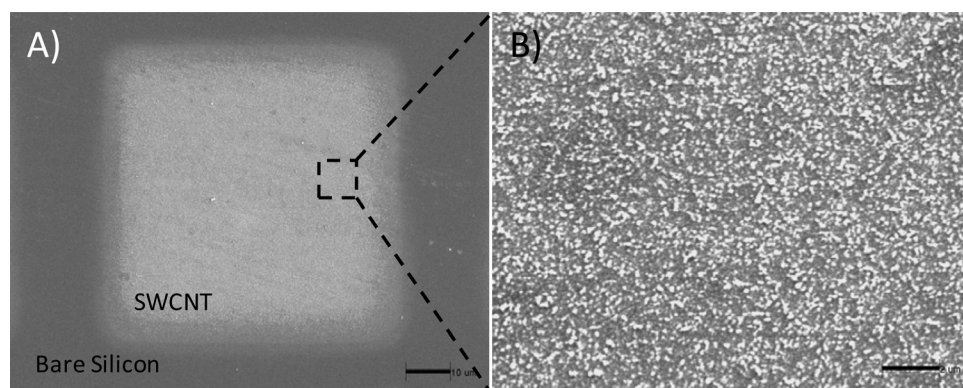|	
1	$e^- + CH_4 \rightarrow CH_3 + H + e^-$
2	$e^- + CH_4 \rightarrow CH_2 + H_2 + e^-$
3	$e^- + CH_4 \rightarrow CH + H_2 + H + e^-$
4	$e^- + CH_4 \rightarrow C + 2H_2 + e^-$

FIG. 2. SEM image of surface after PECVD showing masked areas where no catalyst is present and unmasked where nanotubes have been produced (A), scale bar is 10 μm. Increased magnification of the PECVD surface showing short SWCNT (B), scale bar is 2 μm.

were background subtracted using the WITEC packaged software.

III. RESULTS AND DISCUSSION

A. Scanning electron microscopy

The growth conditions first investigated were 650 °C and 10 min of plasma treatment. To first analyze the substrate after growth SEM was used to image the surface. Figure 2(A) is the SEM image which shows a clear distinction between areas that catalyst was deposited on which subsequently produced SWCNT and the masked areas showing bare silicon. This indicates, as expected, that growth only occurs where iron catalyst particles are deposited. Figure 2(B) is an increased magnification of the SWCNT area showing a rough surface but without discernible tube like features. This would suggest that the nanotubes present are very short and thus difficult to resolve with SEM. Thus it is necessary to use another technique such as Raman to ascertain that indeed SWCNT are present.

B. Raman spectroscopy

To confirm the presence of CNTs when growth is undertaken for 10 min at a temperature of 650 °C and characterize them, confocal Raman microscopy and spectroscopy were

used. In Raman microscopy a Raman spectrum is taken at multiple points across a large area and then the intensity of a peak is plotted. The most intense nanotube specific peaks are the first-order G or graphitic band at $\approx$1590 cm^{-1} which occurs in sp^2 hybridized carbon such as graphite and CNTs and the one-phonon double resonance D or disorder band at 1350 cm^{-1} which alters in intensity depending of number of defects and walls present in CNTs.[19] In the Fig. 3 inset the Raman image (100 $\times$ 100 μm) of the G (or graphitic) band at 1590 cm^{-1} clearly shows the boundary between the masked, where no catalyst exists, and unmasked areas, where SWCNTs are clearly present. This indicates that nanotube growth has occurred only where the iron nanoparticles are present. Figure 3 also compares the Raman spectra of the bare silicon region (dashed line) to the CNT growth region (solid line). The presence of the narrow G band at 1590 cm^{-1} is indicative that sp^2 hybridized carbon has been produced. The intensity of the D and G bands provide a quantitative measure of the level of defects or functionalization present in the SWCNT.[17,18] The average D/G ratio of 0.17 agrees well with other ratios found for high purity SWCNTs. The single sharp peak at 173 cm^{-1} known as the radial breathing mode (or RBM) is well-known to be caused by circumferential expansions that are only present in carbon nanotubes.[19] Due to only a single sharp RBM peak being seen, despite the spot size of the Raman sampling an area of approximately 300 nm in diameter, there must be exceptional
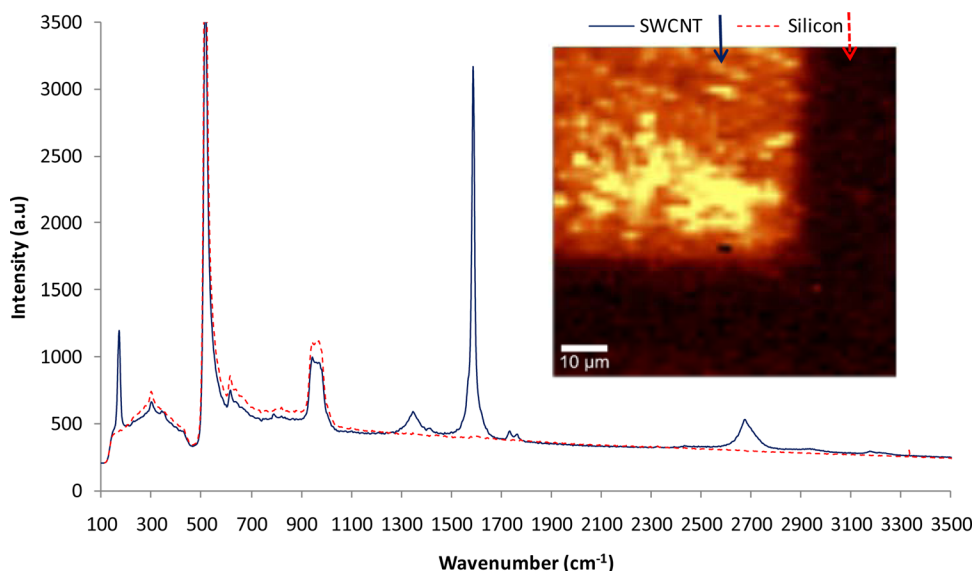

FIG. 3. (Color online) Raman spectra of the substrate showing boundary between areas with catalyst (SWCNT-solid line) and without catalyst (silicon-dashed line). Inset is a 100 $\times$ 100 μm Raman image, plotting the intensity of the G band at 1590 cm^{-1} showing the boundary between the masked and unmasked areas.
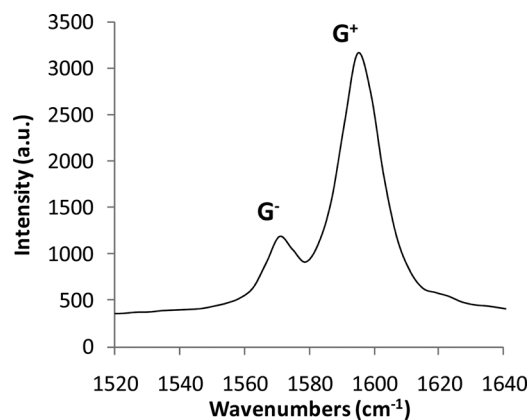
FIG. 4. Enlargement of Raman G band region showing G$^-$ peak at 1570 cm^{-1} and G$^+$ peak at 1590 cm^{-1}, characteristic of semiconducting SWCNT.

homogeneity of the nanotube diameters across the surface. As mentioned previously the RBM is a circumferentially dependent peak, thus its Raman frequency can be used to determine the diameter of the produced nanotubes,[19] the average nanotube diameter across the 50 μm^2 area was found to be 1.47 ± 0.03 nm. The very narrow peak width and high intensity of both the RBM and G band combined with the low intensity of the D peak indicate that high purity tubes with few defects have been produced.

The G peak for the patterned SWCNT also exhibits some further fine structure when enlarged, seen in Fig. 4, where the G peak exists as both a G$^-$ peak at 1570 cm^{-1} and a G$^+$ peak at 1590 cm^{-1}. This is characteristic of SWCNT.[19] Also the relative intensities of these G$^{+/-}$ peaks provides an indication of whether the SWCNTs are semi-conducting or metallic, with a more intense G$^+$ peak, as seen in the
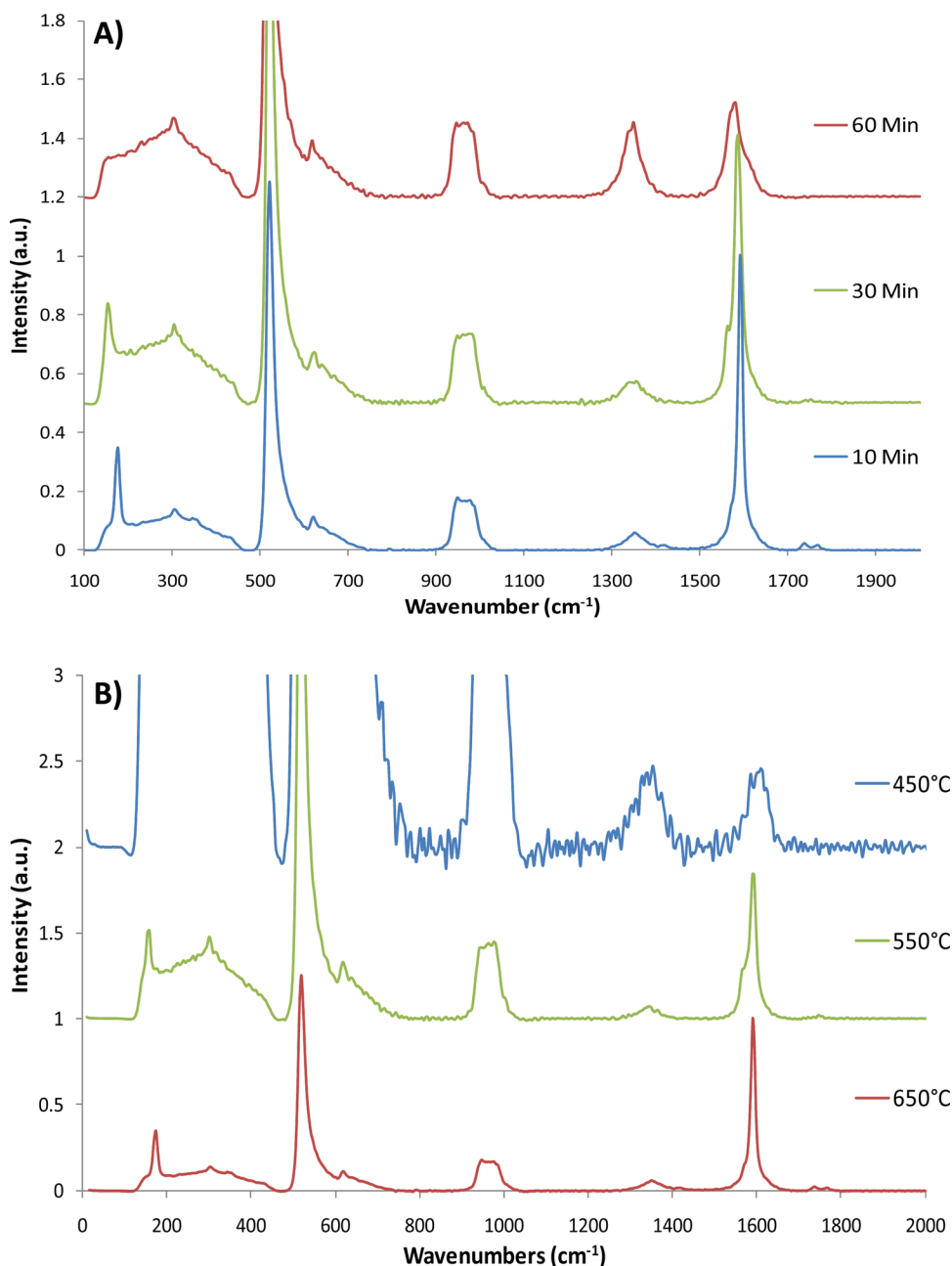

FIG. 5. (Color online) Raman spectra with changing growth time (A) and growth temperature (B).

produced SWCNTs, indicating that semi-conducting SWCNTs have been produced.[24] This may be expected as it has been shown previously that metallic SWCNT undergo selective etching during PECVD, specifically in the presence of methane, leading to preferential semi-conducting nanotube growth.[25] This would be of benefit for applications such as photovoltaics which have shown that semi-conducting nanotubes are needed while metallic nanotubes are detrimental to performance.[4,26,27]

After establishing that SWCNTs can be produced and patterned into defined areas, the growth conditions were then altered to produce different species of nanotube. Figure 5 shows the Raman spectra for changing the growth time and the growth temperature. In Fig. 5(A) we see the Raman spectra with changing growth time. As discussed previously 10 min of growth produces a characteristic SWCNT spectrum, with a clear RBM ($d_t = 1.47$ nm), low D/G ratio and $G^{+/-}$ peak splitting. If the length of time exposed to the plasma is extended to 30 min the spectrum still has SWCNT specific peaks such as the RBM and $G^{+/-}$ splitting; however, the RBM is shifted to a lower frequency of 149 cm^{-1} indicating that the tube diameter has increased to 1.66 nm. As the growth time is further extended to 60 min the spectrum changes significantly, producing no RBM and a D/G ratio of approximately 1, indicating that MWCNTs have been produced. A similar non-linear growth behavior has been observed previously for the production of nanotubes using a cobalt catalyst in the presence of hydrogen and has been attributed to an initial growth of SWCNTs followed by a decrease in the catalytic activity, due to amorphous carbon deposition, of the nanoparticles leading to MWCNT formation.[28] Additionally the SWCNTs are quite fragile and over prolonged time can be preferentially etched away by the plasma.[22] However, MWCNTs are more resistant to plasma etching and so after a prolonged growth exposure only MWCNTs remain. Short growth time also tends to produce a small distribution of nanotube lengths and diameters, as opposed to long growth times that produce large distributions of lengths and diameters, again increasing the chance of MWCNTs being present.[29]

A similar trend is observed in Fig. 5(B) with changing growth temperature. As discussed previously it has been shown that higher temperatures tend to preferentially produce SWCNT and a similar trend is observed here.[18] The 650 °C spectrum is again clearly SWCNT, lowering the temperature to 550 °C lowers the D/G ratio slightly, and the RBM lowers to 156 cm^{-1} indicating a diameter increase to 1.59 nm, but still maintains the SWCNT specific peaks. However, upon lowering the temperature to 450 °C the spectrum clearly changes significantly, again now showing a D/G ratio of approximately 1 and no RBM is observed. The increased noise in the 450 °C spectrum is due to the low intensity of the G peaks against which the spectra have been normalized.

The effect of plasma heating also has to be considered. It has been observed previously that CNT growth can be undertaken without any external heating by the inherent plasma heating of the substrate.[30] However, to achieve the required growth temperature a high plasma density and a DC plasma power of 200 W was required. In this work the use of a much lower plasma density and lower RF power of 10 W would tend to indicate that the effect of plasma heating would be negligible. Indeed if growth is attempted without external heating no carbon nanostructures are achieved. Figure 5 demonstrates how by simply changing one growth variable the resultant CNTs produced can be altered to suit the desired application without the need for large experimental changes.

C. X-ray photoelectron spectroscopy

To complement the Raman data, XPS was performed to analyze the surface of the SWCNT sample. Figure 6 shows the XPS spectra of successive steps during growth. Starting with the bare silicon substrate followed by deposition of the
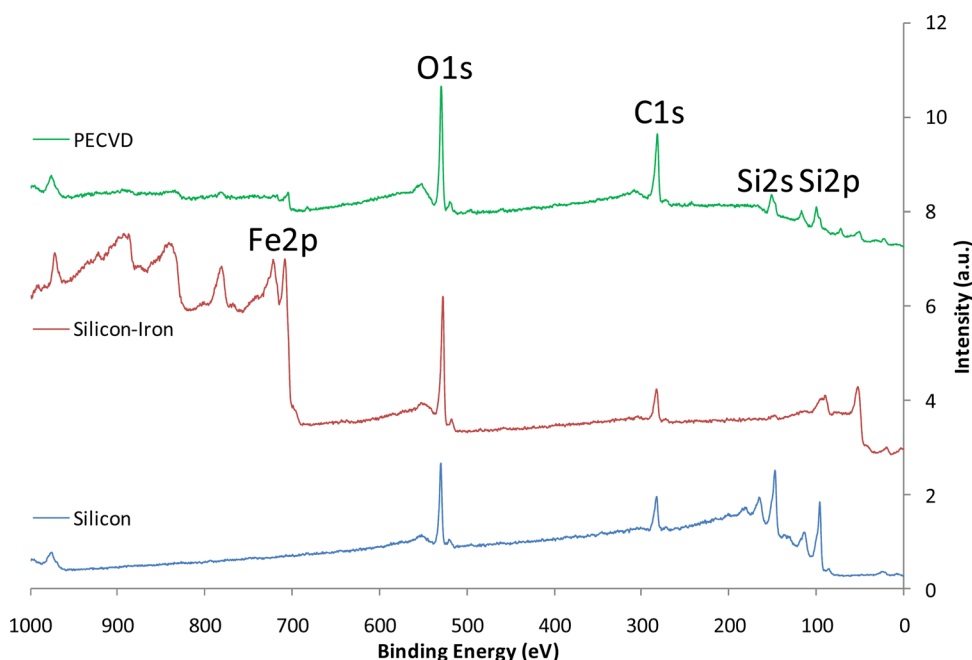

FIG. 6. (Color online) XPS survey spectra for bare silicon, silicon after iron deposition and finally after PECVD growth has occurred.
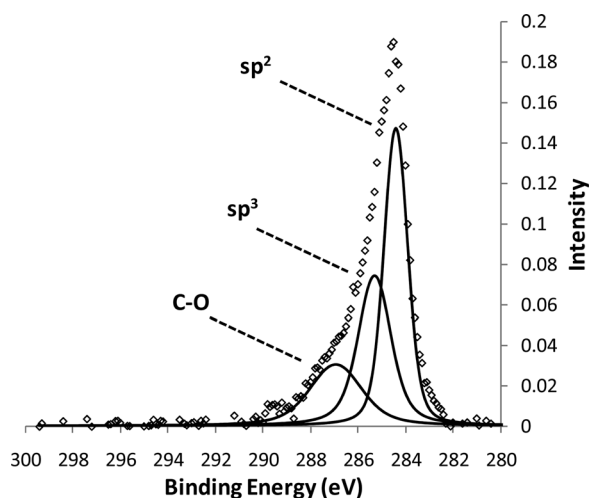
FIG. 7. High resolution XPS spectrum of SWCNT C1s binding region.

5 nm of iron and finally after growth has occurred. Interestingly after growth has been undertaken some iron signal is still present and this may be due to either catalyst particles present on the end of the nanotubes, the so called "tip-growth" process, or more likely is simply due to the low height of the grown nanotube array causing the iron particles at the base to be detected. There is also a small amount of silicon still detectable and this again indicates that the coverage of the surface is not complete and the thickness of the nanotubes remains low.

If the carbon deposited on the surface was amorphous in nature or if the CNTs contained defects in their walls as functional groups, then XPS can determine the extent of any functionality and if so, the specific chemical functionalities present. Figure 7 shows the high resolution scan of the C1s region on a sample of grown SWCNTs from 10 min of growth at 650 °C. The spectrum has been fitted with three components; one at 284.4 eV attributed to sp^2 hybridized carbon, a second peak at 285.2 attributed to sp^3 carbon mainly from adventitious carbon from atmospheric contaminants,[13] and finally a peak at 286.8 eV encompassing oxides of carbon such as carboxyl and carbonyl moieties.[31] The XPS data shows predominantly graphitic carbon is present on the surface, in agreement with the Raman data presented earlier. There is a small amount amorphous or sp^3 hybridized carbon present on the surface, possibly from carbonaceous impurities or possibly defect sites along the CNT walls and end groups. The low amounts of this defective amorphous carbon agree with the D/G ratio seen in the Raman data, indicating high purity. A similar spectrum was taken for the grown MWCNTs after 60 min of growth; however, there was negligible difference as the chemical environment of the carbon is identical in both cases.

IV. CONCLUSION

A simple and tunable method for producing carbon nanotubes in patterned arrays by PECVD has been demonstrated. The transition between SWCNTs and MWCNTs was investigated and appears to be caused by an increased exposure to the growth plasma which leads to decreased catalytic

activity of the iron nanoparticles and preferential etching of SWCNTs leaving a predominantly MWCNT surface. The selective production of high purity semi-conducting SWCNTs was also observed for short growth times. Such nanotubes are vital for use in applications where semi-conducting density of states is necessary, such as photovoltaics. These factors are of importance for any future industrial scale implantation of PECVD grown carbon nanotubes.

[1]C. J. Shearer, J. Yu, K. M. O'Donnell, L. Thomsen, P. C. Dastoor, J. S. Quinton, and J. G. Shapter, J. Mater. Chem. **18**, 5753 (2008).
[2]J. J. Gooding, R. Wibowo, J. Liu, W. Yang, D. Losic, S. Orbons, F. J. Mearns, J. G. Shapter, and D. B. Hibbert, J. Am. Chem. Soc. **125**, 9006 (2003).
[3]B. S. Flavel, D. J. Garrett, J. Lehr, J. G. Shapter, and A. J. Downard, Electrochim. Acta **55**, 3995 (2010).
[4]M. A. Bissett and J. G. Shapter, J. Phys. Chem. C **114**, 6778 (2010).
[5]M. A. Bissett and J. G. Shapter, J. Electrochem. Soc. **158**, K53 (2011).
[6]M. A. Bissett, I. Koper, J. S. Quinton, and J. G. Shapter, Phys. Chem. Chem. Phys. **13**, 6059 (2011).
[7]T. W. Ebbesen and P. M. Ajayan, Nature (London) **358**, 220 (1992).
[8]T. Guo, P. Nikolaev, A. Thess, D. T. Colbert, and R. E. Smalley, Chem. Phys. Lett. **243**, 49 (1995).
[9]K. Hata, D. N. Futaba, K. Mizuno, T. Namai, M. Yumura, and S. Iijima, Science **306**, 1362 (2004).
[10]M. Chhowalla, K. B. K. Teo, C. Ducati, N. L. Rupesinghe, G. A. J. Amaratunga, A. C. Ferrari, D. Roy, J. Robertson, and W. I. Milne, J. Appl. Phys. **90**, 5308 (2001).
[11]R. Hatakeyama *et al.*, J. Phys. D **44**, 174004 (2011).
[12]M. Meyyappan, J. Phys. D **42**, 213001 (2009).
[13]A. Okita, Y. Suda, A. Oda, J. Nakamura, A. Ozeki, K. Bhattacharyya, H. Sugawara, and Y. Sakai, Carbon **45**, 1518 (2007).
[14]G. Zhang, D. Mann, L. Zhang, A. Javey, Y. Li, E. Yenilmez, Q. Wang, J. P. McVittie, Y. Nishi, J. Gibbons, and H. Dai, Proc. Natl. Acad. Sci. USA **102**, 16141 (2005).
[15]M. Meyyappan, L. Delzeit, A. Cassell, and D. Hash, Plasma Sources Sci. Technol. **12**, 205 (2003).
[16]S. Lim, Z. Luo, Z. Shen, and J. Lin, Nanoscale Res. Lett. **5**, 1377 (2010).
[17]E. J. Bae, Y.-S. Min, D. Kang, J.-H. Ko, and W. Park, Chem. Mater. **17**, 5141 (2005).
[18]C. H. Weng, C. S. Yang, H. Lin, C. H. Tsai, and K. C. Leou, J. Nanosci. Nanotechnol. **8**, 2526 (2008).
[19]M. S. Dresselhaus, G. Dresselhaus, R. Saito, and A. Jorio, Phys. Rep. **409**, 47 (2005).
[20]Y. J. Jung, Wei, R. Vajtai, P. M. Ajayan, Y. Homma, K. Prabhakaran, and T. Ogino, Nano Lett. **3**, 561 (2003).
[21]L. Valentini, J. M. Kenny, L. Lozzi, and S. Santucci, J. Appl. Phys. **92**, 6188 (2002).
[22]A. Gohier, T. M. Minea, M. A. Djouadi, and A. Granier, J. Appl. Phys. **101**, 054317 (2007).
[23]M. Mao and A. Bogaerts, J. Phys. D **43**, 205201 (2010).
[24]A. Jorio, M. A. Pimenta, A. G. S. Filho, R. Saito, G. Dresselhaus, and M. S. Dresselhaus, New J. Phys. **5**, 139 (2003).
[25]G. Zhang, P. Qi, X. Wang, Y. Lu, X. Li, R. Tu, S. Bangsaruntip, D. Mann, L. Zhang, and H. Dai, Science **314**, 974 (2006).
[26]T. Schuettfort, A. Nish, and R. J. Nicholas, Nano Lett. **9**, 3871 (2009).
[27]A. D. Pasquier, H. E. Unalan, A. Kanwal, S. Miller, and M. Chhowalla, Appl. Phys. Lett. **87**, 203511 (2005).
[28]A. Gohier, T. M. Minea, A. M. Djouadi, A. Granier, and M. Dubosc, Chem. Phys. Lett. **421**, 242 (2006).
[29]T. Kato and R. Hatakeyama, ACS Nano **4**, 7395 (2010).
[30]K. B. K. Teo, D. B. Hash, R. G. Lacerda, N. L. Rupesinghe, M. S. Bell, S. H. Dalal, D. Bose, T. R. Govindan, B. A. Cruden, M. Chhowalla, G. A. J. Amaratunga, M. Meyyappan, and W. I. Milne, Nano Lett. **4**, 921 (2004).
[31]P. R. Marcoux, J. Schreiber, P. Batail, S. Lefrant, J. Renouard, G. Jacob, D. Albertini, and J.-Y. Mevellec, Phys. Chem. Chem. Phys. **4**, 2278 (2002).